Synthesis and Viscoelastic Behavior of Multiarm Star Polyelectrolytes

Taiichi Furukawa* and Koji Ishizu

Department of Organic Materials and Macromolecules, International Research Center of Polymer Science, Tokyo Institute of Technology, 2-12-1-H133, Ookayama, Meguro-ku, Tokyo 152-8552, Japan

Received October 29, 2004; Revised Manuscript Received January 12, 2005

ABSTRACT: Star-shaped poly(*tert*-butyl acrylate)s were synthesized by the atom transfer radical polymerization (ATRP) method. Subsequently, star-shaped poly(acrylic acid)s were induced by hydrolysis of *tert*-butyl units. The structural ordering of these stars was investigated through small-angle X-ray scattering (SAXS) in aqueous solution. Star with $f = 30$ and $f = 97$ formed a bcc structure above the overlap threshold (C^*). The viscoelastic behavior of the stars was also investigated. This system showed the transition from a Maxwellian fluid of a weak liquid ordering to a solid of macrolattice structure with increasing the polymer concentration. This result reflected the stronger interaction among star polyelectrolytes at higher polymer concentration.

1. Introduction

Star-branched polymers are characterized as structures where all the chains of a molecule are linked together to a small-molar-mass core. Generally, star polymers exhibit smaller hydrodynamic dimensions than the linear polymer with identical molar mass. The interest in star polymers arises not only from the fact that they are models for branched polymers but also from their enhanced segment densities. Zimm and Stockmayer were the first to study the conformation of star-branched polymers using classical theories.[1] Daoud and Cotton studied the conformation and dimensions of star polymers using scaling theories.[2] We have synthesized and investigated the dilute solution properties of polyisoprene (PI) stars. The conformation of those star molecules in good solvents was in agreement with the Daoud−Cotton scaling model of stars. The dilute solution properties suggested that they behaved not as hard spheres but as soft spheres.[3]

Stars with multiarms (the critical number of arms is estimated to be of order 10^2) are expected to form a crystalline array near the overlap threshold (C^*) by Witten et al.[4] We investigated in detail the structural ordering of stars by means of small-angle X-ray scattering (SAXS).[5] PI stars (arm number $f >$ ca. 90) formed a body-centered-cubic (bcc) structure near C^*. This structure changed to a mixed lattice of bcc and face-centered-cubic (fcc) structures with increasing polymer concentration. Recently, we also synthesized functionalized poly(ethylene oxide) (PEO) stars possessing a tertiary amino group at each arm end. Subsequently, positive charges were introduced into such peripheral tertiary amino groups by quarternization with methyl iodide (CH_3I). It was found that these peripherally charged stars ($f > 37$) formed a lattice of bcc below C^* due to electrostatic repulsion between stars.[6] The structure and dynamic behavior of these stars with multiarms have been investigated both in solution[7−10] and in the melt.[8,11] The most interesting features observed in such systems, both in solution and in the melt, relate to the ordering of the stars into a liquidlike structure on the macromolecular scale and the reflection of the latter on the dynamics as an unusual, complex, slow terminal relaxation.[12] In the particular case of melts, this slow process is attributed to star rearrangements within their structure. These effects have been observed both experimentally and in computer-simulated systems.[13,14]

Polyelectrolytes are polymer chains containing ionizable groups. Solution properties of these polymers are different from those uncharged polymers because of dissociation of ionizable groups. Experimental and theoretical studies on the conformation of polyelectrolyte solutions have been undertaken. Recently, conformation and interactions of star-branched polyelectrolyte have also been studied in some detail, using light,[15] neutron,[16] X-ray scattering,[9,17] scaling theory,[18] and computer simulation.[19] Borisov et al.[20] have described a conformation of a single star-branched polyelectrolyte using the self-consistent-field (SCF) approach. They regarded a dilute solution of star-branched polyelectrolytes as an ensemble of spherical cells (analogous to the Wigner−Seitz cell[21]), each containing one star polyelectrolyte molecule localized at the center. The star, whose radius is R, is enclosed in a cell of radius $R_W > R$; all counterions are restricted to move inside this cell. Löwen et al.[22,23] extended this model to the case of concentrated solutions and described the effective interaction of two star polyelectrolytes. The effective interaction between them was ultrasoft in nature but stronger than its counterpart for neutral star polymers.[24] On the other hand, only a few works have reported the behavior of star polyelectrolytes from an experimental point of view. Recently, Heinrich et al.[25] and Moinard et al.[17] investigated the solution properties (structural ordering) of sodium sulfonated polystyrene (PSSNa) stars ($f = 12$) and poly(sodium acrylate) (PANa) stars ($f = 4$) using SAXS. They observed the ordering phenomenon in the neighborhood of the C^*. It is interesting to investigate the correlation between the structural ordering and the dynamics of star polyelectrolytes with multiarms.

In this article, we present the synthesis of poly(acrylic acid) stars with multiarms ($f = 30$, 97). We also investigated the structural ordering and the viscoelastic behavior of these star polyelectrolytes.

2. Experimental Section

Materials. *tert*-Butyl acrylate (*t*BA) and divinylbenzene (DVB) (Tokyo Kasei Ind., Ltd.; 55% m/p-isomer = 2, 45%

10.1021/ma047777n CCC: $30.25
Published on Web 02/19/2005

Table 1. Polymerization Conditions and Results of Star-Shaped p(*t*BA)s[a]

	feed conditions		arm		star				
code	[M] (mmol/L)	[DVB]/[M] (mol/mol)	$10^{-4}\bar{M}_w$[b]	$\bar{M}_w/\bar{M}_n$[b]	$10^{-6}\bar{M}_w$[c]	$\bar{M}_w/\bar{M}_n$	conversion (%)	f	R_c (nm)[d]
$(SM17)_{30}$	30	7	1.7	1.21	0.53	1.09	71.4	30	2.26
$(SM25)_{97}$	20	14	2.5	1.18	2.4	1.12	67.4	97	2.90

[a] All reactions carried out with [macroinitiator]:[CuBr]:[PMDETA] = 1:1:1:1, under high vacuum at 120 °C in *o*-xylene. [b] Determined by GPC using universal calibration on GPC. [c] Determined by SLS in THF. [d] Calculated by $R_c = (3f D_p/4\pi\rho N_A)^{1/3}$. D_p = the degree of polymerization of DVB per one arm; ρ = the density of polystyrene (1.01×10^4 mol/m^3); N_A = Avogado's number.

mixture of ethylstyrene and diethylstyrene) were distilled in high vacuum. Toluene, *o*-xylene, ultrapure water, formic acid, NaOH (Kanto Kagaku, Tokyo), CuBr (Wako Pure Chemical Industries), *N*,*N*,*N*′,*N*′′,*N*′′-pentamethyldiethylenetriamine (PMDETA) (Aldrich), and methyl 2-bromopropionate (Tokyo Kasei, Tokyo) were used as received.

Synthesis Characterization of P(*t*BA) Macroinitiators. Poly(*tert*-butyl acrylate) (p(*t*BA)) macroinitiator was synthesized using CuBr complexed by PMDETA (*N*,*N*,*N*′,*N*′′,*N*′′-pentamethyldiethylenetriamine) as the catalyst and methyl 2-bromopropionate as an initiator in toluene at 80 °C. Subsequently, the reaction solvent was changed to THF after removing toluene using a rotary evaporator and was precipitated in methanol/H_2O (5/5 v/v) after passing through an alumina column to remove the copper complexes. The molecular weight distribution (M_w/M_n) was determined by gel permeation chromatography (GPC; Tosoh high-speed liquid chromatography HLC-8120), which was operated with TSK gel $G2000H_{XL}$ (excluded-limit molecular weight $M_{EL} = 1 \times 10^4$) and two GMH_{XL} columns ($M_{EL} = 4 \times 10^8$), in series using THF as the eluent (flow rate 1.0 mL/min) at 40 °C. The weight-average molecular weight (M_w) was determined by universal calibration[26] ($\log[\eta]M_w$ vs elution volume) by GPC.

Synthesis of P(*t*BA) Star Polymers. P(*t*BA) star polymers were synthesized by polymerization of p(*t*BA) macroinitiator with DVB with CuBr complexed by PMDETA as the catalyst in *o*-xylene at 120 °C. Subsequently, the reaction solvent was changed to THF after removing toluene and was in precipitated in methanol/H_2O (5/5 v/v) after passing through an alumina column to remove the copper complexes. Unreacted p(*t*BA) was removed from the polymerization products by the precipitation fractionation with the THF−H_2O system. The conversion of star polymers was determined by the ratio of the peak of the p(*t*BA) star to the total peak area of the polymerization product in GPC charts. The details concerning the calculation method have been given elsewhere.[27] The arm number f was determined by the ratio of the M_w of the p(*t*BA) star to the $M_{w,arm}$ of the arm.

Hydrolysis of P(*t*BA) Star Polymers. P(*t*BA) star polymer was derived into poly(acrylic acid) (PAA) star polymer by hydrolysis of *t*BA units. P(*t*BA) star polymers were dissolved in the excess of formic acid. The solution was heated at 40 °C for 6 h. The products were diluted in water, dialyzed against water for 2 days, and freeze-dried. The disappearance of *t*BA units was confirmed by ^{1}H nuclear magnetic resonance (NMR; 500 MHz, JEOL GSX-500 NMR spectrometer) in CD_3OD.

Dilute-Solution Properties of Stars. The M_w of the fractionated p(*t*BA) star polymer was determined by static light scattering (SLS: Photal TMLS-6000HL: Otsuka Electronics, $\lambda_0 = 632.8$ nm) in THF at 25 °C in Zimm mode. The scattering angle was in the range of 30°−150°. The RI increment dn/dc (= 0.059 mL/g in THF) of p(*t*BA) star polymer was measured with a differential refractometer (Photal DRM-1021: Otsuka Electronics). Sample solutions were filtered through membrane filters with a nominal pore of 0.2 μm just before measurement.

The diffusion coefficient (D) of p(*t*BA) star polymer was determined by the extrapolation to zero concentration on dynamic light scattering (DLS: Otsuka Electronics) data with cumulant method at 25 °C in THF. The scattering angle was 90°. The hydrodynamic radius (R_H) of PAA star polymer was determined by the CONTIN method on DLS at 25 °C in NaOH aqueous solution.

SAXS Measurement. The SAXS intensity distribution was measured with a rotating-angle X-ray generation (Rigaku Denshi Rotaflex RTP300RC) operated at 40 kV and 100 mA. The X-ray source was monochromatized to Cu Kα ($\lambda = 1.5418$ Å) radiation. In the measurement of the solution sample, a glass capillary ($\phi = 2.0$ mm, Mark-Röhrchen Ltd.) was used as a holder vessel. The SAXS patterns were taken with a fine-focused X-ray source using a flat plate camera (Rigaku Denki, RU-100). The SAXS intensity profiles plotted from the horizontal section of the SAXS patterns without considering the smearing correction.

Rheological Measurements. The measurements were performed in an ARES rheometer (Rheometric Scientific) using a cone−plate geometry ($\phi = 25$ mm, cone angle = 0.04 rad). Dynamic frequency sweep measurements were performed in the linear viscoelastic regime, as determined previously by dynamic strain sweep measurements. Concentrated solutions were prepared by evaporating the water from diluted solution under vacuum. The polymer concentration was gravimetrically calculated. The solutions were transparent.

3. Results and Discussion

Synthesis and Dilute-Solution Properties of P(*t*BA) Stars. Controlled/"living" radical polymerization processes have proven to be versatile for the synthesis of polymer with well-defined structures. Several comprehensive reviews for controlled/"living" radical polymerization have been published.[28−31] We synthesized star polymers by the atom transfer radical polymerization (ATRP) method. Table 1 lists polymerization conditions and results for p(*t*BA) star polymers. In no case were cross-linked or insoluble materials observed. It is well-known that the apparent polydispersity of branched polymer is smaller than that of the linear polymer. Therefore, this effect would be reflected the results that the polydispersity of the star polymer is smaller than that of the arm polymer. Figure 1 shows typical GPC profiles of SM25 and the polymerization product $(SM25)_{97}$. The GPC peak at lower elution volume in RI chart corresponds to the p(*t*BA) star polymer. The GPC elution pattern of the second peak is identical with that of SM25. Then, the polymerization product $(SM25)_{97}$ is a mixture of p(*t*BA) star polymer and unreacted p(*t*BA) homopolymer. The conversion of star polymer was 67.4%. Here, the radius of core (R_c) was estimated by assumed that the density of poly(divinylbenzene) was equal to that of polystyrene because the yield of the star and the feed amounts of DVB were known. We calculated the R_c from the equation $R_c = (3f D_P/4\pi\rho N_A)^{1/3}$, where ρ is the density of polystyrene (1.01×10^4 mol/m^3), N_A is Avogadro's number, and D_p is the degree of the polymerization of the DVD (including ethylstyrene) per one arm molecule. These physical values were also shown in Table 1. Each star (SM-F) was removed from the corresponding unreacted p(*t*BA) homopolymer by the precipitation fractionation with a THF−water system (see Figure 1). For example, the sample code $(SM25)_{97}$F means M_w of arm = 2.5×10^4 and arm number = 97.

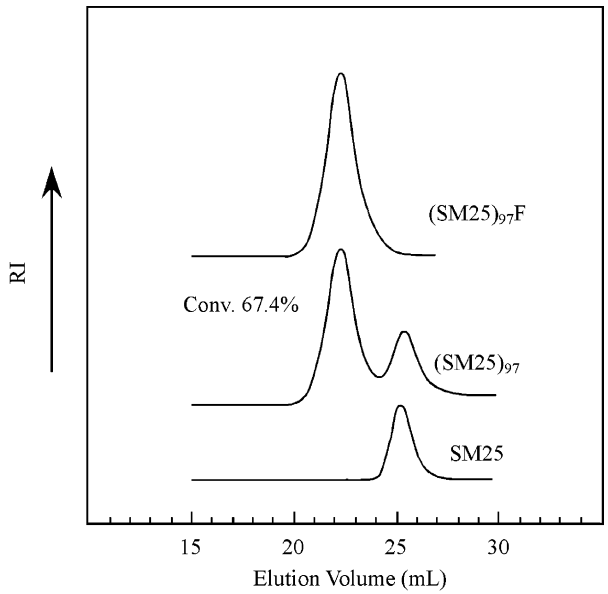

Figure 1. GPC profiles of star-shaped p(*t*BA) star $(SM25)_{97}$, fractionated star $(SM25)_{97}F$, and macroinitiator SM25.

Table 2. Characteristics of Star-Shaped Poly(*tert*-butyl acrylate)s

code	$10^{-6}\bar{M}_w$[b]	$\bar{M}_w/\bar{M}_n$[a]	$10^{-4}\bar{M}_{w,arm}$[a]	f	R_G (nm)[b]	R_H (nm)[c]	R_G/R_H
$(SM17)_{30}F$	0.53	1.09	1.7	30	17.1	14.5	1.18
$(SM25)_{97}F$	2.4	1.12	2.5	97	23.2	20.0	1.16

[a] Determined by GPC using universal calibration on GPC. [b] Determined by SLS in THF. [c] Determined by DLS in THF.

We examined the dilute-solution properties of p(*t*BA) star polymers using SLS and DLS in THF at 25 °C. The observed physical values of p(*t*BA) star polymers are listed in Table 2. The mutual diffusion coefficient $D(c)$ had an almost constant value against the polymer concentration. As observed in $(AB)_n$ star block,[32] prototype,[33] and double-cylinder-type copolymer brushes,[34] p(*t*BA) star polymers also formed a single molecule in THF. The translational diffusion coefficient D can be estimated by extrapolation of polymer concentration to zero. The hydrodynamic radius (R_H) can be estimated by the Stokes−Einstein equation $R_H = kT/6\pi\eta_0 D$, where k, T, and η_0 indicate Boltzmann coefficient, absolute temperature, and viscosity of solvent, respectively. The ratio R_G/R_H is a sensitive fingerprint of the inner density profile of star molecules and polymer micelles. The values of R_G/R_H for stars were in the range 1.16−1.18. It is well-known that R_G/R_H for unperturbed polymers and hard spheres with uniform density are 1.25−1.37[35] and 0.775,[36] respectively. It is concluded that p(*t*BA) star polymers behave not as hard spheres but as soft spheres in dilute solution.

Dilute-Solution Properties of PAA Star Polymers. The *tert*-butyl ester groups were hydrolyzed using excess of formic acid. The hydrolysis seemed to proceed almost perfectly from the disappearance of the proton signal for the *tert*-butyl groups.

In recent years, Borisov et al.[18] describe the conformation of weak star-branched polyelectrolytes in dilute solution and the dependence of the overall star size on the number of branches. Thus, we examined the dynamics of PAA star polymers in dilute solution by varying solution pH. Here, we define the normalized first-order correlation function for the scattered electric field $g^{(1)}(\tau)$ from the sample, where τ is time. In a DLS measurement, we obtain the second-order correlation function, $g^{(2)}(\tau)$. The two correlation functions are linked via the Siegert relation

$$g^{(2)} = 1 + |g^{(1)}(\tau)|^2 \quad (1)$$

If the scattering medium has only one relaxation mode, $g^{(2)}(\tau) - 1$ is simply given one exponential functions. PAA star polymers with different numbers of charge are measured. For $(SMA25)_{97}F$ star, the stars in pH 4.0, 6.6, and 7.6 solutions are neutralized 0, 50, and 80 mol % charges, respectively. Figure 2 shows the plots of the translational diffusion coefficient $D(c)$ as a function of the polymer concentration (Figure 2a) and the correlation function at 90° scattering angle for $(SMA25)_{97}F$ in pH 4.0 solution. The diffusion coefficient $D(c)$ had an almost constant value against the polymer concentration. Also, the correlation function at various scattering angles showed the identical one exponential decay to that measured at 90° scattering angle. These results indicate the absence of intermolecular interactions and aggregation. For branched polyelectrolyte such as stars, most of the counterions are trapped inside the stars while the concentration of counterions in the interstar regions is considerably smaller than the average value. This can be shown by direct measurement of the osmotic pressure of the counterions of salt-free solutions of the spherical polyelectrolyte brushes by Ballauff et al.[37] Groenewegen et al.[38,39] have also reported the counterions distribution in the coronal layer of polyelectrolyte diblock copolymer micelles by means of the SANS experiment. Löwen et al.[24] showed that the counterions above ca. 85% were trapped within arm polymer by using molecular dynamics (MD) computer simulation. They also found the tendency of the star polyelectrolyte to increase the fraction of absorbed counterions as f and/or degree of dissociation α increase. Therefore, the constant value of $D(c)$ and one exponential correlation function for PAA star polymer should mean the weak polyelectrolyte effect of interchain interactions. Hence, the measured D_H derived from the diffusion coefficient shows narrow size distribution (Figure 2c) and reflects the hydrodynamic dimension of PAA star polymer. These PAA star polymers are expected to behave as soft spheres as well as nonionic star polymers. The softness of PAA stars is discussed in the next section. The observed physical values of 80 mol % charged PAA star polymers are listed in Table 3.

Structural Ordering of PAA Star Polymers. The structural ordering of 80 mol % charged PAA star polymers was investigated by means of SAXS in salt-free aqueous solution, varying the polymer concentration. The ionic strength was kept constant for the different polymer concentration. We measured first the SAXS intensity profiles of the $(SMA25)_{97}F$ star at 4.7, 8.0, and 9.4 wt % of aqueous polymer solutions. These polymer concentrations were higher than the C^* (1.6 wt %). Figure 3 shows SAXS intensity profiles for the $(SMA25)_{97}F$, where q [= $(4\pi/\lambda)\sin\theta$] (where θ is one-half the scattering angle) is the magnitude of the scattering vector. The arrows and the values in parentheses indicate the scattering maxima and interplanar spacing (d_1/d_n), respectively, calculated from the Bragg reflection. At 4.7 wt % of polymer concentration (Figure 3a), the first five peaks appear closely at the relative q positions of $1:\sqrt{2}:\sqrt{3}:\sqrt{4}:\sqrt{5}$, as shown in parentheses. The interplanar spacing (d_1/d_n) at the scattering angles

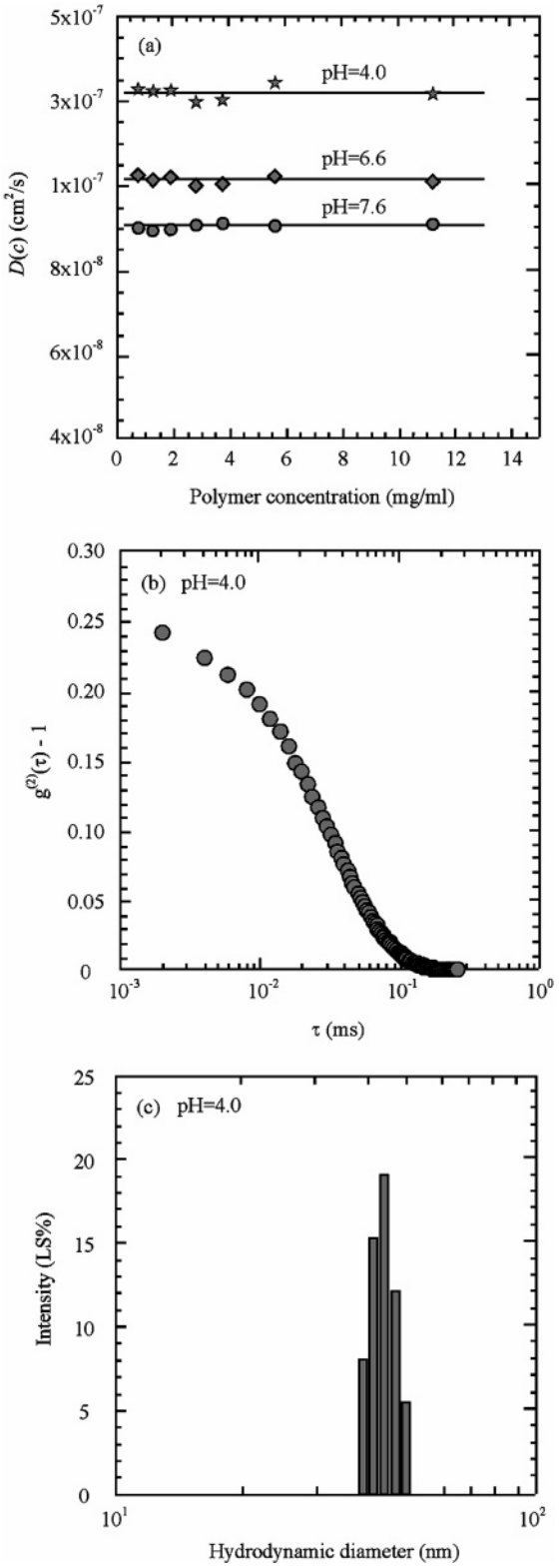

Figure 2. (a) Plots of translational diffusion coefficient $D(c)$ as a function of the polymer concentration for $(SMA25)_{97}F$. (b) Plot of correlation function for $(SMA25)_{97}F$. (c) Size distribution for $(SMA25)_{97}F$.

is relative to the angle of the first maximum according to Bragg's equation: $2d \sin \theta = n\lambda$ (where $\lambda = 1.5418$ Å). These values correspond to the packing pattern of (110), (200), (211), (220), and (310) planes in a bcc structure. Similar lattice patterns are also observed in the SAXS profiles at 8.0 and 9.4 wt % of the polymer concentration (Figure 3b,c). It is noticed that the first

Table 3. Characteristics of Star-Shaped Poly(acrylic acid)s

code	$10^{-6}\bar{M}_w$	f	R_H (nm)[a]	C^* (wt %)[b]
$(SM17)_{30}F$	0.32	30	25.0	14.5
$(SM25)_{97}F$	1.7	97	35.0	20.0

[a] Determined by DLS in aqueous solution. [b] Calculated by the equation $C^* = 3\bar{M}_w/4\pi R_H^3 N_A$.

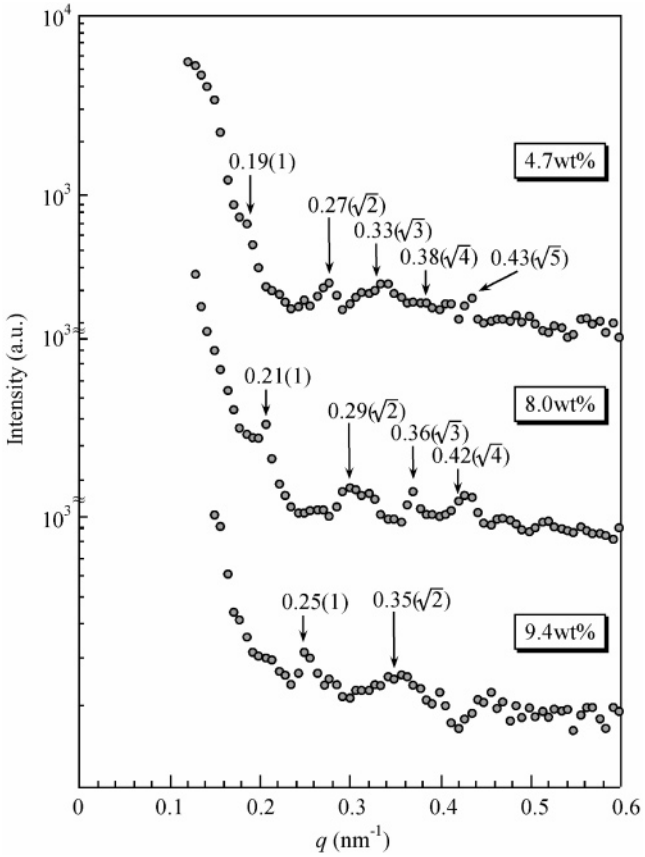

Figure 3. SAXS intensity profiles for $(SMA25)_{97}F$: 4.7, 8.0, and 9.4 wt %.

peak shift to the side of high q position in the order of the increment of the polymer concentration. This fact means that Bragg spacing d_1 became shorter with increasing the polymer concentration.

The result of SAXS data obtained for $(SMA17)_{30}F$ star was almost the same as that for the $(SMA25)_{97}F$ star. That is to say, the structural ordering such as a bcc lattice appeared above C^*, and the packing density increased with increasing the polymer concentration.

We consider spatial packing of the cubic lattice in aqueous solution. The measured Bragg spacing d_1 is related to the cell edge a_c of the cubic lattice and the nearest-neighbor distance of the spheres D_0:

$$D_0 = (\sqrt{3/2})a_c = \sqrt{(3/2)}d_1 \quad \text{for bcc} \qquad (2)$$

Table 4 lists the physical values on spatial packing of the cubic lattice for 80 mol % charged $(SMA17)_{30}F$ and $(SMA25)_{97}F$. We carried out the double-logarithmic plot of D_0 as a function of polymer concentration. It is found that the measured D_0 is proportional to the -0.34th power of the polymer concentration and fits well with the $-1/3$ power expected for the homogeneous system. This fact means that the spherical particles of

Table 4. Physical Values on Spatial Packing of Cubic Lattices in Aqueous Solution

	polymer concn (wt %)	q_1 (nm^{-1})	d_1 (nm)[a]	D_0 (nm)[b]
$(SM17)_{30}F$	4.8	0.19	33.0	40.5
	7.9	0.22	28.5	35.0
	9.1	0.26	24.1	29.6
	11.5	0.30	20.9	25.6
$(SM25)_{97}F$	4.7	0.19	33.0	40.5
	8.0	0.21	29.9	36.6
	9.4	0.25	25.1	30.7

[a] Calculated by $d_1 = 2\pi/q_1$. [b] Calculated by $D_0 = (\sqrt{3/2})d_1$.

PAA stars lead to isotropic shrinkage with increasing the polymer concentration due to the softness of PAA stars.

Rheological Measurements Figure 4 shows the flow curves of 80 mol % charged $(SMA25)_{97}F$ in salt-free aqueous solutions at the polymer concentrations of 4.7, 8.0, and 9.4 wt %. With increasing the polymer concentration, the change of the flow behavior is observed. At 5.0 wt % of the polymer concentration, Newtonian flow is observed. The shear stress, σ, is proportional to the shear rate, $d\gamma/dt$, as follows

$$\sigma = \eta \frac{d\gamma}{dt} \tag{3}$$

and the viscosity $\eta = 49.2$ mPa·s. This means that the interactions between the star polymers are very weak, and the system is a homogeneous solution under shearing. On the other hand, at 8.0 wt % of the polymer concentration, non-Newtonian flow behavior is observed. The rheological behavior in the plastic flow region indicates the presence of a solidlike structure responsible for a yield stress. The flow behavior with yield stress $\sigma_0 = 190$ Pa for 9.4 wt % was observed (see Figure 4c). Similar rheological transition were observed for $(SMA17)_{30}F$. It is interesting that the changes in viscoelasticity by varying the polymer concentration. The dependence of the yield stress on the polymer concentration and the comparison with hard spheres and other colloidal systems would be very important, but this information has been left unsolved in this work.

Figure 5 shows the frequency, ω, dependence of the storage modulus, G', and the loss modulus, G'', of $(SMA25)_{97}F$ in aqueous solutions at the polymer concentrations of 4.7, 8.0, and 9.4 wt %. At 4.7 wt % of the polymer concentration (Figure 5a), G' and G'' exhibit typical behavior for viscoelastic (Maxwellian) fluids. That is, G' scales with ω^2 and G'' does ω^1. On the other hand, for 8.0 wt % of the polymer concentration (Figure 5b), the crossover between G' and G'' is observed at $\omega_c = 10$ rad/s. This indicates that the system at this concentration becomes a viscoelastic fluid with a long relaxation time at this frequency. At a higher frequency than this critical frequency ($\omega_c = 10$ rad/s), the system behaves as a solid. However, for $\omega < \omega_c$, it is a viscous solution and flows. For 9.4 wt % of the polymer concentration (Figure 5c), G' has a larger modulus than G'' in the overall range of frequencies. These results indicate that the structural transition from a weak liquid ordering structure to a macrolattice structure is by way of like a sol−gel transition. Similar behavior was observed for $(SMA17)_{30}F$, which shows the tendency that the value of the storage modulus increased with increasing the polymer concentration. The value of the storage modulus would reflect the strength of the interaction between star polyelectrolytes.

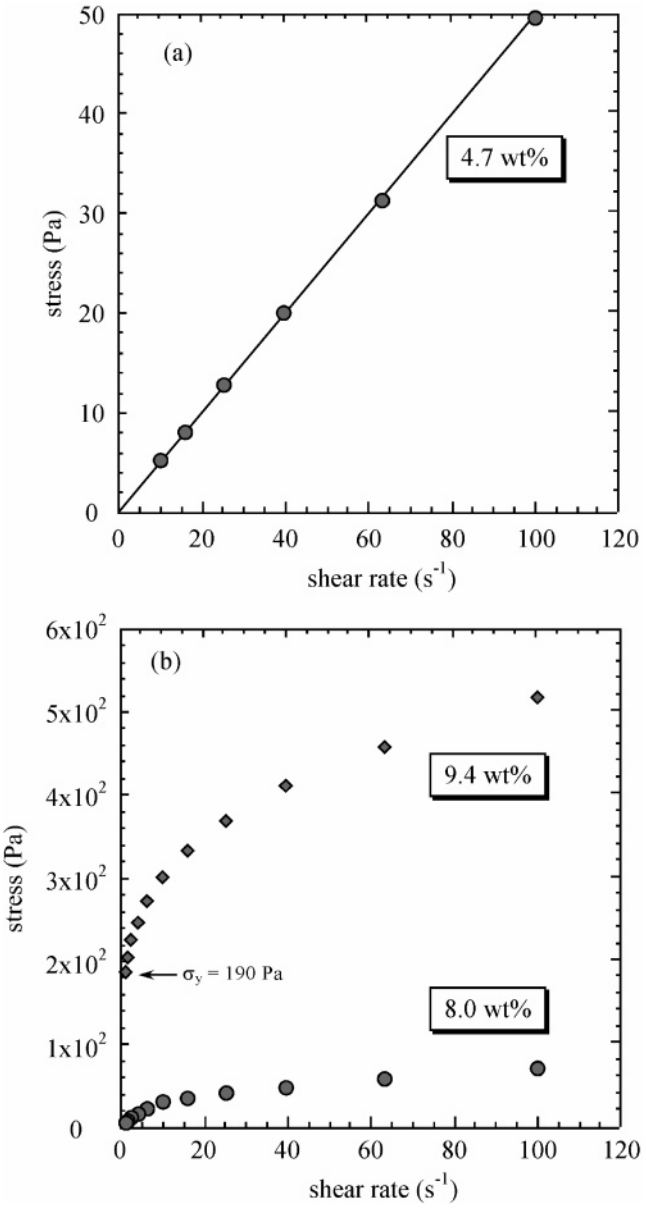

Figure 4. Flow behavior of $(SMA25)_{97}F$: (a) 4.7, (b) 8.0, and 9.4 wt %.

As mentioned in the Introduction, Löwen et al.[24] have examined the effective interactions of star polyelectrolytes using molecular dynamics (MD) simulations with analytical theory. More recently, Jusufi et al.[40] showed the simplified effective interaction between two spherical polyelectrolyte brushes. They neglected the tiny fraction of charge outside of the brush and presented the effective interaction $V_{eff}(D)$ between two spherical polyelectrolyte brushes, kept at center-to-center distance D, as follows:

$$\frac{V_{eff}(D)}{k_B T} = \frac{Q}{|e|}\left[\frac{1}{2RK}\left(D \ln^2\left(\frac{D}{2R}\right) + 8R_c \ln\left(\frac{R_c}{R}\right)\right) + \ln\left(\frac{2L}{RK}\right) - 2\frac{R_c}{L}\ln\left(\frac{R_c}{R}\right)\right] \tag{4}$$

where R is the radius of the star, R_c is the radius of the core, $L = R - R_c$, and K is a D-dependent dimensionless parameter obtained from the condition $\int_{V_{in}} \rho(r)\, d^3r = Q$,

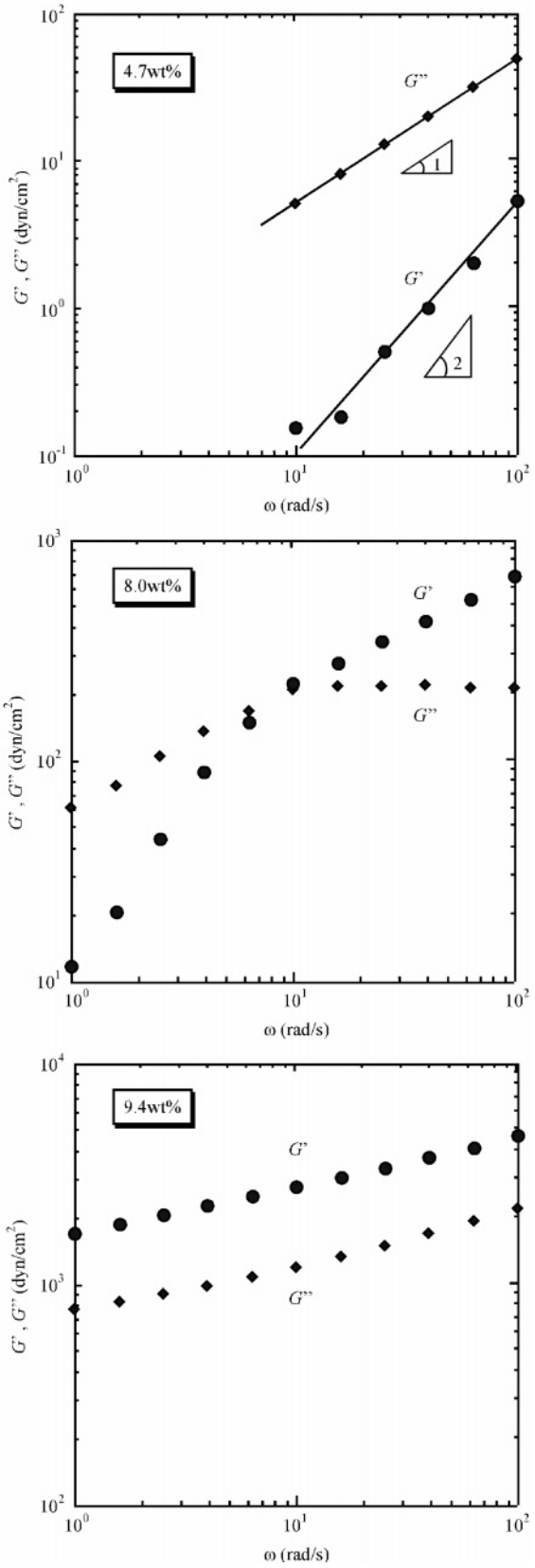

Figure 5. Viscoelastic behavior of $(SMA25)_{97}F$ at various polymer concentrations.

where $\rho(r) = A/r^2$ and the normalization factor $A = Q/(4\pi R\mathrm{K})$. This yields

$$K = 1 - 2\frac{R_c}{R} + \frac{D}{2R}\left[1 - \ln\left(\frac{D}{2R}\right)\right] \qquad (5)$$

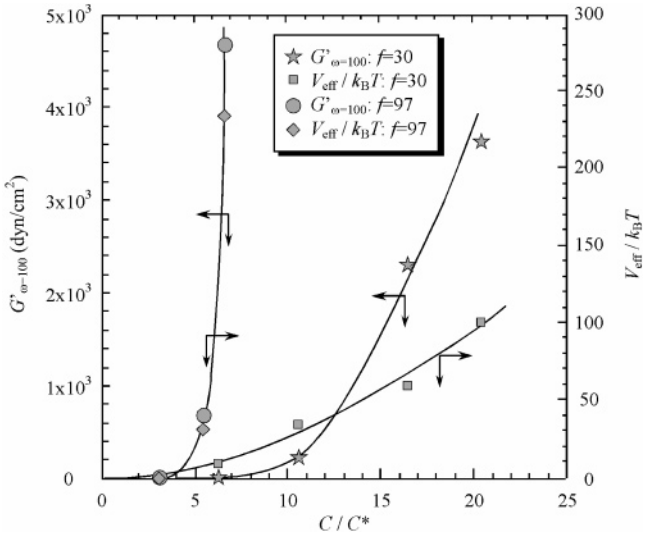

Figure 6. Plots of the $G'_{\omega=100}$ and V_{eff} as a function of C/C^*.

In our case, because the star polyelectrolytes carry a very high charge (almost every monomer along the chain is charged), we expect a significant number of counterions to be cylindrically condensed along the rodlike chains. A simple estimate of the number of condensed counterions can be obtained by considering the Manning parameter, ξ, which is defined as the ratio of the Bjerrum length $\lambda_B = e^2/(\epsilon k_B T)$ (where ϵ denotes the dielectric constant of the solvent, k_B is Boltzmann's constant, and T is the absolute temperature) to the distance a between two sequential charged sites. With the Bjerrum length $\lambda_B = 7.1$ Å (corresponding to water at 25 °C), we obtain for the Manning parameter the value $\xi = (\lambda_B/a) \approx 3$. This implies that the number of condensed counterions is $Q_{\mathrm{cond}} = Q_{\mathrm{bare}}(1 - 1/\xi)$, approximately two-thirds of the bare charge. As the bare charge is roughly $Q_{\mathrm{bare}} = 3.5 \times 10^4|e|$ for $(SMA17)_{30}F$ and $1.9 \times 10^5|e|$ for $(SMA25)_{97}F$, the effective charge $Q = 1.2 \times 10^4|e|$ and $6.3 \times 10^4|e|$, respectively. The effective interaction between star polyelectrolyte was calculated by using R_c (from Table 1), R_H (from Table 3), and D_0 (from Table 4). Figure 6 shows the plots of the storage modulus $G'_{\omega=100}$ and the effective interaction V_{eff} as a function of C/C^*. It is found from this figure that $G'_{\omega=100}$ and V_{eff} of $(SMA25)_{97}F$ diverge for $C/C^* < 6$. On the other hand, gradual increasing of $G'_{\omega=100}$ and V_{eff} of $(SMA15)_{30}F$ can be seen. This type of behavior has been discussed with nonionic stars. Likos et al. have proposed the effective pair potential $V(r)$ between two nonionic star polymers.[41] The stars with $f < 64$ show only gradual increasing of $V(r)$. For high $f = 128$ and 256, however, $V(r)$ diverges like colloidal particles. This result for nonionic star agrees with our results. Namely, $(SMA15)_{30}F$ PAA star would behave like a nonionic star polymer due to decreasing of the effective charge with increasing the polymer concentration. Therefore, $G'_{\omega=100}$ and V_{eff} of $(SMA15)_{30}F$ PAA star would result in gradual increasing for $C/C^* < 20$. This speculation may be verified by adding salt to monitor transition from polyelectrolyte to nonionic behavior. We believe that these star polyelectrolytes offer a new soft colloidal system with many opportunities for tuning their behaviors. As the rheological data presented are rather limited, however, they are only preliminary. A complete rheological investigation is currently under way and will be reported in the near future.

4. Conclusions

Star-shaped poly(*tert*-butyl acrylate)s were synthesized by the atom transfer radical polymerization (ATRP) method. Subsequently, star-shaped poly(acrylic acid)s were induced by hydrolysis of *tert*-butyl units. The structural ordering of these stars was investigated through small-angle X-ray scattering (SAXS) in aqueous solution. Star with $f = 30$ and $f = 97$ formed a bcc structure above the overlap threshold (C^*). The nearest-neighbor distance of the spheres (D_0) decreased continuously with increasing the polymer concentration. The viscoelastic behavior of the stars was also investigated. This system showed the transition from a Maxwellian fluid of a weak liquid ordering to a solid of macrolattice structure with increasing the polymer concentration. The effective interaction between two star polyelectrolytes was evaluated by using Löwen's prediction. It was found that the effective interaction has stronger dependence on the polymer concentration with increasing the arm number.

References and Notes

(1) Zimm, B. H.; Stockmayer, W. H. *J. Chem. Phys.* **1949**, *17*, 1301.
(2) Daoud, M.; Cotton, J. P. *J. Phys. (Paris)* **1982**, *43*, 531.
(3) Ishizu, K.; Ono, T.; Uchida, S. *Macromol. Chem. Phys.* **1997**, *198*, 3255.
(4) Witten, T. A.; Pincus, P. A.; Catea, M. A. *Europhys. Lett.* **1986**, *2*, 137.
(5) Ishizu, K.; Ono, T.; Uchida, S. *J. Colloid Interface Sci.* **1997**, *192*, 189.
(6) Furukawa, T.; Ishizu, K. *Macromolecules* **2003**, *36*, 434.
(7) Seghrouchni, R.; Petekidis, G.; Vlassopoulos, D.; Fytas, G.; Semenov, A. N.; Roovers, J.; Fleischer, G. *Europhys. Lett.* **1998**, *42*, 271.
(8) Vlassopoulos, D.; Fytas, G.; Roovers, J.; Pakula, T.; Fleischer, G. *Faraday Discuss.* **1999**, *112*, 225.
(9) Semenov, A. N.; Vlassopoulos, D.; Fytas, G.; Vlachos, G.; Fleischer, G.; Roovers, J. *Langmuir* **1999**, *15*, 358.
(10) Vlassopoulos, D.; Kapnistos, M.; Fytas, G.; Roovers, J. *Macromol. Symp.* **2000**, *158*, 149.
(11) Vlasspoulos, D.; Pakula, T.; Fytas, G.; Roovers, J.; Karatasos, K.; Hadjichristidis, N. *Europhys. Lett.* **1997**, *39*, 617.
(12) Roovers, J. *J. Non-Cryst. Solids* **1991**, *131*−*133*, 793.
(13) Vlassopoulos, D.; Fytas, G.; Pakula, T.; Roovers, J. *J. Phys.: Condens. Matter* **2001**, *13*, R855.
(14) Pakula, T. *Comput. Theor. Polym. Sci.* **1998**, *8*, 21.
(15) Sedlak, M. *Langmuir* **1999**, *15*, 4045.
(16) Boue, F.; Cotton, J. P.; Lapp, A.; Jannink, G. *J. Chem. Phys.* **1994**, *101*, 2562.
(17) Moinard, D.; Taton, D.; Gnanou, Y.; Rochas, C.; Borsali, R. *Macromol. Chem. Phys.* **2003**, *204*, 89.
(18) Borisov, O. V.; Zhulina, E. B. *Eur. Phys. J. B* **1998**, *4*, 205.
(19) Roger, M.; Guenoun, P.; Muller, F.; Belloni, L.; Delsanti, M. *Eur. Phys. J. E* **2002**, *9*, 313.
(20) Wolterink, J. K.; Leermakers, F. A. M.; Fleer, G. J.; Koopal, L. K.; Zhulina, E. B.; Borisov, O. V. *Macromolecules* **1999**, *32*, 2365.
(21) Zimam, J. M. *Models of Disorder*; Cambridge University Press: Cambridge, UK, 1979.
(22) Jusufi, A.; Likos, C. N.; Löwen, H. J. *Phys. Rev. Lett.* **2002**, *88*, 018301.
(23) Likos, C. N.; Hoffmann, N.; Jusufi, A.; Löwen, H. J. *J. Phys.: Condens. Matter* **2003**, *15*, S233.
(24) Jusufi, A.; Likos, C. N.; Löwen, H. *J. Chem. Phys.* **2002**, *116*, 11011.
(25) Heinrich, M.; Rawiso, M.; Zilliox, J. G.; Lesieur, P.; Simon, J. P. *Eur. Phys. J. E* **2001**, *4*, 131.
(26) Grubisic, Z.; Rempp, P.; Benoit, H. *J. Polym. Sci., Part B* **1967**, *5*, 753.
(27) Ishizu, K.; Shimomura, K.; Saito, R.; Fukutomi, T. *J. Polym. Sci., Polym. Chem. Ed.* **1991**, *29*, 607.
(28) Kamigaito, M.; Ando, T.; Sawamoto, M. *Chem. Rev.* **2001**, *101*, 3689.
(29) Matyjaszewski, K.; Xia, J. *Chem. Rev.* **2001**, *101*, 2921.
(30) Coessens, V.; Pintauer, T.; Matyjaszewski, K. *Prog. Polym. Sci.* **2001**, *26*, 337.
(31) Qiu, J.; Charleux, B.; Matyjaszewski, K. *Prog. Polym. Sci.* **2001**, *26*, 2083.
(32) Ishizu, K.; Uchida, S. *Prog. Polym. Sci.* **1999**, *24*, 1439.
(33) Tsubaki, K.; Kobayashi, H.; Satoh, J.; Ishizu, K. *J. Colloid Interface Sci.* **2001**, *241*, 275.
(34) Tsubaki, K.; Ishizu, K. *Polymer* **2001**, *42*, 8287.
(35) Roovers, J.; Martin, J. E. *J. Polym. Sci., Part B: Polym. Phys.* **1989**, *27*, 2513.
(36) Antonietti, M.; Gremser, W.; Schmidt, M. *Macromolecules* **1990**, *23*, 3796.
(37) Das, B.; Guo, X.; Ballauff, M. *Prog. Colloid Polym. Sci.* **2003**, *121*, 34.
(38) Groenewegen, W.; Egelhaaf, S. U.; Lapp, A.; van der Maarel, J. R. C. *Macromolecules* **2000**, *33*, 3283.
(39) Groenewegen, W.; Lapp, A.; Egelhaaf, S. U.; van der Maarel, J. R. C. *Macromolecules* **2000**, *33*, 4080.
(40) Jusufi, A.; Likos, C. N.; Ballauff, M. *Colloid Polym. Sci.* **2004**, *282*, 910.
(41) Likos, C. N.; Löwen, H.; Watzlawek, M.; Abbas, B.; Jucknischke, O.; Allgaier, J.; Richter, D. *Phys. Rev. Lett.* **1998**, *80*, 4450.

MA047777N